Acta Mech 229, 4131–4139 (2018)
https://doi.org/10.1007/s00707-018-2226-z

ORIGINAL PAPER

Sergey V. Kuznetsov

Lamb waves in functionally graded plates with transverse inhomogeneity

Received: 20 April 2018 / Revised: 21 June 2018 / Published online: 30 July 2018

Abstract Propagation of harmonic Lamb waves in plates made of functionally graded materials with transverse inhomogeneity is studied by the modified Cauchy six-dimensional formalism. For arbitrary transverse inhomogeneity, a closed-form dispersion equation is derived. Dispersion relations for materials with different kinds of inhomogeneity are obtained and compared.

1 Introduction

Functionally graded materials (FGMs) with continuous transverse inhomogeneity can considerably change acoustical properties of functionally graded (FG) plates resulting in either filtering of some kinds of acoustic waves at particular frequencies [1], or considerably changing dispersion curves and the corresponding dispersion relations [2–5]. These properties of wave propagation in FGM plates are of particular interest in various NDT applications [6,7].

In most works on acoustic wave propagation in FG plates, various numerical approaches are suggested. One of the modifications of FEM, known as the "strip FEM" was used in [1]; in [5] the hybrid FEM was used for modeling fundamental modes of Lamb waves in FG plates. In [9,10], a spectral variant of FEM was used to obtain dispersion curves in FG rods. Legendre polynomials and the accompanying functions were used in [11] for constructing dispersion relations for Lamb waves in FG plates. Peano series expansions for analyzing dispersion of piezoelectric FG plates were exploited in [8]. Asymptotic methods based on WKB (Wentzel–Kramers–Brillouin) technique for analyzing dispersion of Lamb modes in FG plates were suggested in [12].

The present work is devoted to constructing explicit secular equation and the corresponding (implicit) solution by the Cauchy six-dimensional formalism, previously developed for analysis of Lamb waves in *homogeneous* stratified plates [13]. Herein, only traction-free boundary conditions are considered. Numerical examples are also presented revealing some peculiarities in the dispersion curves of the fundamental symmetric modes of Lamb waves in FG plates.

It should also be mentioned that as the literature review shows, the developed method is currently the only theoretical method for analyzing dispersion of Lamb waves propagating in anisotropic FG plates with no restriction on elastic anisotropy and transverse inhomogeneity.

2 Governing equations

Herein, the main equations for constructing the solution for Lamb waves in a functionally graded plate are derived.

S. V. Kuznetsov (✉)
Institute for Problems in Mechanics, Russian Academy of Sciences, Moscow, Russia
E-mail: kuzn-sergey@yandex.ru

2.1 Equations of motion and Lamb wave representation

The linear equations of motion for anisotropic inhomogeneous material can be written in the form

$$\mathrm{div}\mathbf{C}(\mathbf{x}) \cdot \cdot \nabla \mathbf{u}(\mathbf{x}, t) = \rho(\mathbf{x})\ddot{\mathbf{u}}(\mathbf{x}, t) \tag{2.1}$$

where double dots "$\cdot\cdot$" stand for convolution in two indices; $\mathbf{u}$ is the displacement field; $\mathbf{x}$ is the position vector; t is time; ρ is the material density; and $\mathbf{C}(\mathbf{x})$ is the fourth-order elasticity tensor assumed to be strongly elliptic:

$$\underbrace{\forall \mathbf{x}}_{\mathbf{x}\in\mathbb{R}^3} \quad \underbrace{\forall \mathbf{m}, \mathbf{n}}_{\mathbf{m},\mathbf{n}\in\mathbb{R}^3,\mathbf{m},\mathbf{n}\neq 0} \quad \mathbf{m} \otimes \mathbf{n} \cdot \cdot \mathbf{C}(\mathbf{x}) \cdot \cdot \mathbf{n} \otimes \mathbf{m} > 0 \tag{2.2}$$

and $\mathbf{C}(\mathbf{x}) \in C^1(\mathbb{R}^3)$, i.e., $\mathbf{C}(\mathbf{x})$ is continuously differentiable in $\mathbb{R}^3$.

Hereafter, the propagation of a harmonic Lamb wave in a plate with transverse inhomogeneity is specified by the transverse dimensionless complex coordinate

$$x = ir\mathbf{x} \cdot \boldsymbol{\nu}, \tag{2.3}$$

where "$\cdot$" stands for the scalar product; $\boldsymbol{\nu}$ is the unit normal to the median plane; r is the wave number having dimension l^{-1} and $i = \sqrt{-1}$; see Fig. 1. Origin of the global coordinate system belongs to the median plane Π_ν.

The following wave representation for the Lamb wave is adopted:

$$\mathbf{u}(\mathbf{x}, t) = \mathbf{m}(x)e^{ir(\mathbf{n}\cdot\mathbf{x}-ct)}, \tag{2.4}$$

where $\mathbf{m}$ is the (unknown) variation of the vector wave amplitude across the thickness of the plate; $\mathbf{n}$ is the unit vector indicating the direction of propagation; c is the phase velocity of the Lamb wave and is independent of the direction.

Substituting representation (2.4) into the equations of motion yields

$$\left(\mathbf{A}_1(x)\frac{\mathrm{d}^2}{\mathrm{d}x^2} + \mathbf{A}_2(x)\frac{\mathrm{d}}{\mathrm{d}x} + \mathbf{A}_3(x)\right) \cdot \mathbf{m}(x) = 0, \tag{2.5}$$

where

$$\begin{aligned}
\mathbf{A}_1(x) &= \boldsymbol{\nu} \cdot \mathbf{C}(x) \cdot \boldsymbol{\nu}, \\
\mathbf{A}_2(x) &= \boldsymbol{\nu} \cdot \left(\frac{\mathrm{d}\mathbf{C}(x)}{\mathrm{d}x}\right) \cdot \boldsymbol{\nu} + \boldsymbol{\nu} \cdot \mathbf{C}(x) \cdot \mathbf{n} + \mathbf{n} \cdot \mathbf{C}(x) \cdot \boldsymbol{\nu}, \\
\mathbf{A}_3(x) &= \boldsymbol{\nu} \cdot \left(\frac{\mathrm{d}\mathbf{C}(x)}{\mathrm{d}x}\right) \cdot \mathbf{n} + \mathbf{n} \cdot \mathbf{C}(x) \cdot \mathbf{n} - \rho(x)c^2\mathbf{I}.
\end{aligned} \tag{2.6}$$

In Eqs. (2.6), $\mathbf{A}_1(x)$ is the acoustical tensor and $\mathbf{I}$ denotes the unit diagonal 3×3-matrix. Note that the strong ellipticity condition (2.2) ensures

$$\det \mathbf{A}_1(x) > 0 \tag{2.7}$$

and

$$\det \mathbf{A}_3(x) > 0 \tag{2.8}$$

provided c satisfies the following condition:

$$c < \sqrt{\frac{\lambda_3}{\rho(x)}}, \tag{2.9}$$

where λ_3 is the smallest eigenvalue of the tensor: $\boldsymbol{\nu} \cdot \left(\frac{\mathrm{d}\mathbf{C}(x)}{\mathrm{d}x}\right) \cdot \mathbf{n} + \mathbf{n} \cdot \mathbf{C}(x) \cdot \mathbf{n}$. Hereafter, it is assumed that condition (2.9) is satisfied.

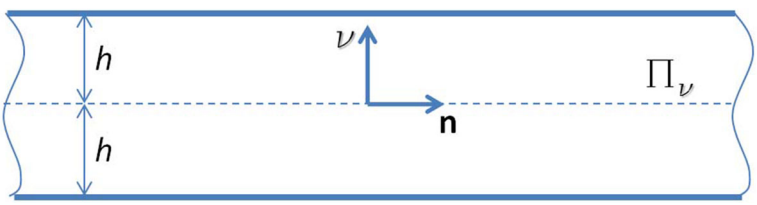

Fig. 1 Plate of thickness $2h$; unit vectors $\mathbf{n}$ and $\boldsymbol{\nu}$ indicate direction of propagation and normal to the median plane Π_ν, respectively

2.2 Six-dimensional Cauchy formalism

Introducing a new vector wave amplitude

$$\mathbf{w}(x) = \frac{\mathrm{d}}{\mathrm{d}x}\mathbf{m}(x) \tag{2.10}$$

yields equations of motion in terms of two unknown vector amplitudes $\mathbf{m}$ and $\mathbf{w}$:

$$\begin{aligned} &\frac{\mathrm{d}}{\mathrm{d}x}\mathbf{m}(x) = \mathbf{w}(x), \\ &\frac{\mathrm{d}}{\mathrm{d}x}\mathbf{w}(x) = -\mathbf{A}_1^{-1}(x)\cdot\mathbf{A}_3(x)\cdot\mathbf{m}(x) - \mathbf{A}_1^{-1}(x)\cdot\mathbf{A}_2(x)\cdot\mathbf{w}(x), \end{aligned} \tag{2.11}$$

where it is assumed that the acoustical tensor $\mathbf{A}_1(x)$ is invertible.

Introducing a new six-dimensional amplitude

$$\mathbf{Y}(x) = \begin{pmatrix} \mathbf{m}(x) \\ \mathbf{w}(x) \end{pmatrix} \tag{2.12}$$

allows us to rewrite Eqs. (2.11) in the following form:

$$\frac{\mathrm{d}}{\mathrm{d}x}\mathbf{Y}(x) = \mathbf{G}(x)\cdot\mathbf{Y}(x), \tag{2.13}$$

where $\mathbf{G}(x)$ is a six-dimensional matrix:

$$\mathbf{G}(x) = \begin{pmatrix} \mathbf{0} & \mathbf{I} \\ -\mathbf{A}_1^{-1}(x)\cdot\mathbf{A}_3(x) & -\mathbf{A}_1^{-1}(x)\cdot\mathbf{A}_2(x) \end{pmatrix}. \tag{2.14}$$

Herein, "$\cdot$" stands for matrix multiplication; $\mathbf{0}$ is a 3×3-matrix with zero components. Equation (2.13) is the main equation of the Cauchy formalism, and the matrix $\mathbf{G}$ will be called fundamental matrix. Conditions (2.2) and (2.9) ensure

$$\det\mathbf{G}(x) = \det\mathbf{A}_1^{-1}(x)\det\mathbf{A}_3(x) > 0. \tag{2.15}$$

2.3 Boundary conditions

Traction-free boundary conditions have the form

$$\mathbf{t}_\nu(\mathbf{x},t) \equiv \boldsymbol{\nu}\cdot\mathbf{C}(x)\cdot\cdot\nabla\mathbf{u}(\mathbf{x},t)|_{x=\pm irh} = 0, \tag{2.16}$$

where the plate thickness is $2h$ (Fig. 1). Substituting the representation (2.4) into the boundary conditions (2.16) with account of the notations (2.6), (2.10) yields

$$\mathbf{A}_1(x)\cdot\mathbf{w}(x) + \mathbf{A}_4(x)\cdot\mathbf{m}(x)|_{x=\pm irh} = 0, \tag{2.17}$$

where

$$\mathbf{A}_4(x) = \boldsymbol{\nu}\cdot\mathbf{C}(x)\cdot\mathbf{n}. \tag{2.18}$$

Finally, the conditions (2.17) can be rewritten in terms of the vector $\mathbf{Y}(x)$:

$$\mathbf{t}_\nu(x) \equiv (\mathbf{A}_4(x), \mathbf{A}_1(x))\cdot\mathbf{Y}(x)|_{x=\pm irh} = 0. \tag{2.19}$$

2.4 Matrix equation

Let $\mathbf{E}$ be a matrix satisfying Eq. (2.13):

$$\frac{\mathrm{d}}{\mathrm{d}x}\mathbf{E}(x) = \mathbf{G}(x) \cdot \mathbf{E}(x). \tag{2.20}$$

The matrix $\mathbf{E}$ is assumed to be non-degenerate, i.e., $\det \mathbf{E} \neq 0$.

If such a matrix exists, then any vectorial solution $\mathbf{Y}(x)$ of Eq. (2.13), due to the linearity of the problem, takes the form

$$\mathbf{Y}(x) = \mathbf{E}(x) \cdot \vec{C}, \tag{2.21}$$

where $\vec{C}$ is a six-dimensional vector of unknown coefficients, defined by the boundary conditions (2.16).

Equation (2.20) can obviously be rewritten in the equivalent form

$$\left(\frac{\mathrm{d}}{\mathrm{d}x}\mathbf{E}(x)\right) \cdot \mathbf{E}^{-1}(x) = \mathbf{G}(x). \tag{2.22}$$

2.5 Matrix solution

Applying matrix function analysis [14] allows the construction of a matrix solution for Eq. (2.22) in the form

$$\mathbf{E}(x) = e^{\mathbf{F}(x)+\mathbf{A}}, \tag{2.23}$$

where

$$\mathbf{F}(x) \equiv \int \mathbf{G}(x)\mathrm{d}x \tag{2.24}$$

stands for an indefinite integral of $\mathbf{G}(x)$. It will be shown that the arbitrary constant matrix appearing in Eq. (2.23) does not affect the final result.

Direct verification reveals that the matrix (2.23) satisfies Eq. (2.22). The right-hand side of expression (2.23) shows that matrix $\mathbf{E}(x)$ is non-degenerate for the phase velocity satisfying condition Eqs. (2.9), that is due to (2.15), Now, combining Eqs. (2.21) and (2.23), the vector-valued general solution $\mathbf{Y}$ can be constructed.

3 Dispersion equation

Substituting the general solution at $x = +irh$ into the representation (2.21) with account of (2.12) yields

$$\mathbf{E}(x) \cdot \vec{C}\Big|_{x=+irh} = \mathbf{Y}(irh), \tag{3.1}$$

from where

$$\vec{C} = \mathbf{E}^{-1}(irh) \cdot \mathbf{Y}(irh). \tag{3.2}$$

Equation (3.1) yields

$$\mathbf{Y}(-irh) = \mathbf{E}(-irh) \cdot \underbrace{\mathbf{E}^{-1}(irh) \cdot \mathbf{Y}(irh)}_{\vec{C}=\mathbf{E}^{-1}\cdot\mathbf{Y}}. \tag{3.3}$$

The following 6×6 matrix is needed for the subsequent analysis:

$$\mathbf{Z}(x) = \begin{pmatrix} \mathbf{I} & \mathbf{0} \\ \mathbf{A}_4(x) & \mathbf{A}_1(x) \end{pmatrix}. \tag{3.4}$$

Note, that the matrix $\mathbf{Z}(x)$ is invertible at any x, since $\det \mathbf{Z} = \det \mathbf{A}_1 > 0$ due to the strong ellipticity condition (2.2). Thus, the matrix $\mathbf{Z}(x)$ can be considered as one-to-one mapping in $\mathbb{R}^6$, and taking into account (2.12), (2.19),

$$\begin{pmatrix} \mathbf{m}(x) \\ \mathbf{t}_v(x) \end{pmatrix} = \mathbf{Z}(x) \cdot \begin{pmatrix} \mathbf{m}(x) \\ \mathbf{w}(x) \end{pmatrix}. \tag{3.5}$$

Now, both surface displacement magnitude $\mathbf{m}$ and surface traction $\mathbf{t}_v$ at $x = -irh$ can be written in terms of the matrix $\mathbf{Z}$ and the expressions (3.3) and (3.5) as

$$\begin{pmatrix} \mathbf{m}(-irh) \\ \mathbf{t}_v(-irh) \end{pmatrix} = \mathbf{T}(irh) \cdot \begin{pmatrix} \mathbf{m}(irh) \\ \mathbf{t}_v(irh) \end{pmatrix}, \tag{3.6}$$

where

$$\mathbf{T}(irh) \equiv \mathbf{Z}(-irh) \cdot \mathbf{E}(-irh) \cdot \mathbf{E}^{-1}(irh) \cdot \mathbf{Z}^{-1}(irh). \tag{3.7}$$

Useful for computation purposes formula comes from analyzing the composition $\mathbf{E}(-irh) \cdot \mathbf{E}^{-1}(irh)$, revealing

$$\mathbf{E}(-irh) \cdot \mathbf{E}^{-1}(irh) = e^{\mathbf{F}(-irh) - \mathbf{F}(irh)} = \exp\left(- \int\limits_{-irh}^{irh} \mathbf{G}(x) \mathrm{d}x \right). \tag{3.8}$$

Thus, composition $\mathbf{E}(-irh) \cdot \mathbf{E}^{-1}(irh)$ does not contain an arbitrary (constant) matrix $\mathbf{A}$; see Eq. (2.23).

Since the surface traction fields in (3.6) vanish at $x = \pm irh$, the following 3×3 matrix operator

$$\mathbf{B} \equiv (\mathbf{0}, \mathbf{I}) \cdot \mathbf{T} \cdot \begin{pmatrix} \mathbf{I} \\ \mathbf{0} \end{pmatrix} \tag{3.9}$$

from the 3D space of surface displacements and vanishing surface tractions on the "upper" surface to the 3D space of surface tractions on the "bottom" surface should be degenerate to ensure existence of a non-trivial displacement magnitude on the "upper" surface resulting in vanishing surface tractions on the "bottom" surface. The latter equation is equivalent to

$$\det\left((\mathbf{0}, \mathbf{I}) \cdot \mathbf{T} \cdot \begin{pmatrix} \mathbf{I} \\ \mathbf{0} \end{pmatrix} \right) = 0. \tag{3.10}$$

Equation (3.10) is the desired dispersion equation for a plate with free boundaries. The dispersion equation (3.10) coincides with one obtained for a *homogeneous* anisotropic plate [13].

4 Special cases

Here, two special kinds are considered.

4.1 Homogeneous anisotropy

It is supposed that both the elasticity tensor and the material density are homogeneous,

$$\mathbf{C}(x) = \mathbf{C}_0, \quad \rho(x) = \rho_0, \tag{4.1}$$

where $\mathbf{C}_0$ is the fourth-order strongly elliptic tensor, and $\rho_0 > 0$ is the material density.

Substituting (4.1) into Eqs. (2.6), (2.14) yields the fundamental matrix $\mathbf{G}_0$ independent of the exponential multiplier $e^{\lambda \cdot x}$, $\mathbf{G}(x) = \mathbf{G}_0$. Thus, for the considered case, the fundamental solution of Eq. (2.20) takes the form

$$\mathbf{E}(x) = e^{\mathbf{G}_0 x}. \tag{4.2}$$

And due to the assumed homogeneity condition (4.1), the matrix defined by Eq. (3.4) is independent of x, so $\mathbf{Z}(x) = \mathbf{Z}_0$ and the transfer matrix $\mathbf{T}$ contains the argument irh accounting for dispersion only within the term

$$\mathbf{E}(-irh) \cdot \mathbf{E}^{-1}(irh) = e^{-2irh\mathbf{G}_0}. \tag{4.3}$$

Now, due to (4.3), the dispersion relation (3.10) for a homogeneous plate becomes

$$\det\left((\mathbf{0}, \mathbf{I}) \cdot \mathbf{Z}_0 \cdot e^{-2irh\mathbf{G}_0} \cdot \mathbf{Z}_0^{-1} \cdot \begin{pmatrix} \mathbf{I} \\ \mathbf{0} \end{pmatrix} \right) = 0. \tag{4.4}$$

4.2 Exponential inhomogeneity

Now, it is assumed that both the elasticity tensor and the material density have an exponential inhomogeneity

$$\mathbf{C}(x) = \mathbf{C}_0 e^{\lambda x}, \quad \rho(x) = \rho_0 e^{\lambda x}, \tag{4.5}$$

where $\mathbf{C}_0$ is the fourth-order strongly elliptic tensor, and $\rho_0 > 0$. Note, that due to Eq. (2.3) the exponent factor λ should be imaginary to ensure real values for both $\mathbf{C}(x)$ and $\rho(x)$.

Substituting Eqs. (4.5) into Eqs. (2.6) yields

$$\begin{aligned}
\mathbf{A}_1(x) &= (\boldsymbol{\nu} \cdot \mathbf{C}_0 \cdot \boldsymbol{\nu})\, e^{\lambda x}, \\
\mathbf{A}_2(x) &= (\lambda \boldsymbol{\nu} \cdot \mathbf{C}_0 \cdot \boldsymbol{\nu} + \boldsymbol{\nu} \cdot \mathbf{C}_0 \cdot \mathbf{n} + \mathbf{n} \cdot \mathbf{C}_0 \cdot \boldsymbol{\nu})\, e^{\lambda x}, \\
\mathbf{A}_3(x) &= \left(\lambda \boldsymbol{\nu} \cdot \mathbf{C}_0 \cdot \mathbf{n} + \mathbf{n} \cdot \mathbf{C}_0 \cdot \mathbf{n} - \rho_0 c^2 \mathbf{I}\right) e^{\lambda x}.
\end{aligned} \tag{4.6}$$

Substituting Eqs. (4.6) into Eq. (2.14) yields the fundamental matrix independent of the exponential factor $e^{\lambda x}$. However, in view of Eq. $(4.6)_2$, the fundamental matrix depends upon the exponent multiplier λ, thus $\mathbf{G}(x) = \mathbf{G}_0(\lambda)$. Now, the fundamental (matrix) solution of Eq. (2.20) or (2.22) takes the form

$$\mathbf{E}(x) = e^{\mathbf{G}_0(\lambda) x}. \tag{4.7}$$

The expressions (2.18), (4.6) yield the matrix $\mathbf{Z}(x)$:

$$\mathbf{Z}(\lambda x) = \begin{pmatrix} \mathbf{I} & 0 \\ (\boldsymbol{\nu} \cdot \mathbf{C}_0 \cdot \mathbf{n})\, e^{\lambda x} & (\boldsymbol{\nu} \cdot \mathbf{C}_0 \cdot \boldsymbol{\nu})\, e^{\lambda x} \end{pmatrix}. \tag{4.8}$$

Thus, for the considered case of exponential homogeneity, the matrix $\mathbf{Z}(x)$ contains the dispersive terms due to the presence of multipliers $e^{\lambda x}$. With (4.8), the inverse matrix $\mathbf{Z}^{-1}(x)$ becomes

$$\mathbf{Z}^{-1}(\lambda x) = \begin{pmatrix} \mathbf{I} & 0 \\ -(\boldsymbol{\nu} \cdot \mathbf{C}_0 \cdot \boldsymbol{\nu})^{-1} \cdot (\boldsymbol{\nu} \cdot \mathbf{C}_0 \cdot \mathbf{n}) & (\boldsymbol{\nu} \cdot \mathbf{C}_0 \cdot \boldsymbol{\nu})^{-1}\, e^{-\lambda x} \end{pmatrix}. \tag{4.9}$$

The constructed matrices yield the dispersion equation (3.10) in the form

$$\det\left((\mathbf{0}, \mathbf{I}) \cdot \mathbf{Z}(-irh\lambda) \cdot e^{-2irh\mathbf{G}_0(\lambda)} \cdot \mathbf{Z}^{-1}(irh\lambda) \cdot \begin{pmatrix} \mathbf{I} \\ \mathbf{0} \end{pmatrix} \right) = 0. \tag{4.10}$$

5 Examples

While the theory, developed in Sect. 3, refers to the general heterogeneous anisotropy, herein, an *isotropic* FGM plate with transverse heterogeneity is analyzed. The dispersion curves for the considered FGM plate are compared with ones for the corresponding *homogenized isotropic* plates.

5.1 FGM plate

Consider an isotropic FGM plate with the following physical properties:

$$E(x) = E_0 \frac{(1 + \alpha \cosh(i\beta x))}{2}, \nu = \text{const.}, \rho = \text{const.}, \tag{5.1}$$

where E_0 corresponds to Young's modulus at the median plane $x = 0$ at $\alpha \neq 0$; here α and $\beta \neq 0$ are dimensionless real-valued constants; x is the dimensionless imaginary coordinate; $\nu \in (-1; 0.5)$ is the Poisson ratio, ρ is the material density. The inequality

$$\alpha > -\frac{1}{\cosh(\beta h)} \tag{5.2}$$

ensures that $E(x) > 0$ at $-ih < x < +ih$. For the considered FGM plate, both the Poisson ratio and the material density are assumed constant with respect to depth.

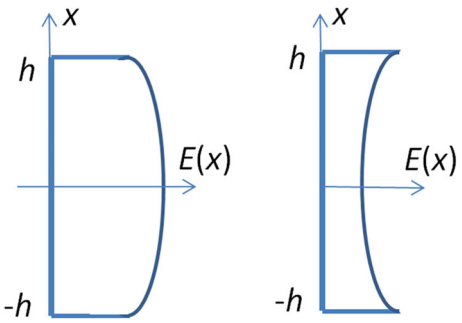

Fig. 2 Variation of Young's modulus with depth: left ($\alpha > 0$); right ($\alpha < 0$)

Depending on the sign of the constant α, Young's modulus variation with depth is ether convex ($\alpha > 0$) or concave ($\alpha < 0$); see Fig. 2:

With the elastic constants (5.1), the components of the elasticity tensor become

$$C_{ijkl}(x) = \lambda(x)\delta_{ij}\delta_{kl} + \mu(x)\left(\delta_{ik}\delta_{jl} + \delta_{il}\delta_{ik}\right), \tag{5.3}$$

where δ_{ij} is the Kronecker delta, and λ, μ are Lamé constants:

$$\lambda(x) = \frac{E(x)\nu}{(1+\nu)(1-2\nu)}; \quad \mu(x) = \frac{E(x)}{2(1+\nu)}. \tag{5.4}$$

With account of Eqs. (5.3), (5.4), the equations (2.6) become

$$\begin{aligned}
\mathbf{A}_1(x) &= (\lambda(x) + 2\mu(x))\,\mathbf{v}\otimes\mathbf{v},\\
\mathbf{A}_2(x) &= \left(\frac{d\,(\lambda(x)+2\mu(x))}{dx}\mathbf{v}\otimes\mathbf{v} + (\lambda(x)+\mu(x))\,(\mathbf{v}\otimes\mathbf{n} + \mathbf{n}\otimes\mathbf{v})\right),\\
\mathbf{A}_3(x) &= \frac{d\lambda(x)}{dx}\mathbf{v}\otimes\mathbf{n} + \frac{d\mu(x)}{dx}\mathbf{n}\otimes\mathbf{v} + (\lambda(x)+2\mu(x))\,\mathbf{n}\otimes\mathbf{n} - \rho_0 c^2\mathbf{I}.
\end{aligned} \tag{5.5}$$

5.2 Homogenized plate

Along with the FGM plate, a plate with homogenized properties is also considered with averaged Young's modulus (E_{hom})

$$E_{\text{hom}} \equiv \frac{E_0}{2}\left(1 + \frac{\alpha}{2ih}\int_{-ih}^{ih}\cosh(i\beta x)\mathrm{d}x\right) = \frac{E_0}{2}\left(1 + \frac{\alpha}{\beta h}\sinh(\beta h)\right). \tag{5.6}$$

As the right-hand side of Eq. (5.6) shows, $E_{\text{hom}} > E_0/2$ at $\alpha > 0$, and $E_{\text{hom}} < E_0/2$ at $\alpha < 0$.

5.3 Dispersion curves

The following nondimensional numerical values for the parameters (5.1) were adopted:

$$E_0 = 1; \quad \alpha = \pm 0.5; \quad \beta = 1; \quad \nu = 0.25; \quad \rho = 1; \quad h = 1. \tag{5.7}$$

Direct verification shows that the condition (5.2) is satisfied for these numerical values. For the parameters (5.7), Eq. (5.6) yields: $E_{\text{hom}} \approx 0.794$ at $\alpha = 0.5$ and $E_{\text{hom}} \approx 0.206$ at $\alpha = -0.5$.

Applying the method developed in Sect. 3 and substituting the isotropic elasticity tensor defined by (5.3) with the material constants (5.7) allows us to plot dispersion curves for the considered FGM and homogenized plates in terms of nondimensional phase speed c vs. nondimensional frequency ω; see Fig. 3.

Comparing the plotted dispersion curves for the considered symmetric fundamental modes reveals:

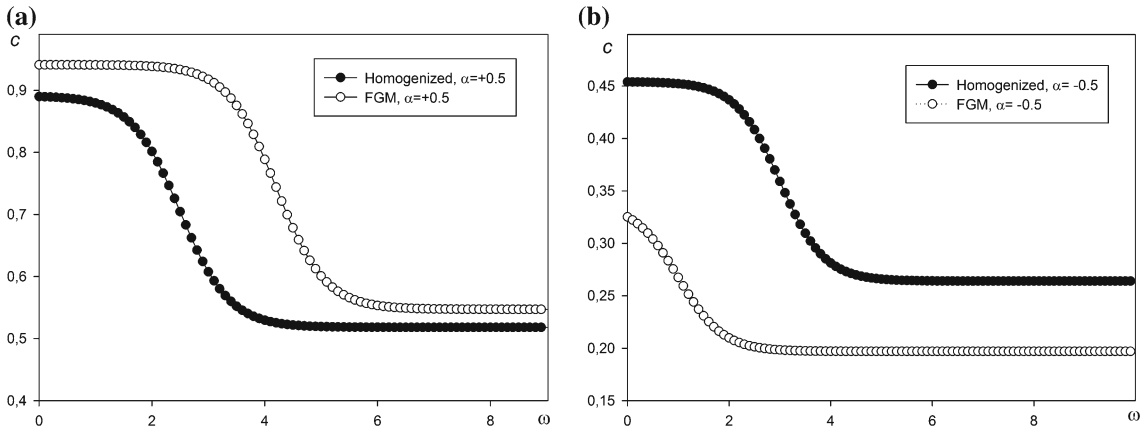

Fig. 3 Dispersion curves related to the fundamental symmetric Lamb modes: **a** $\alpha = +0.5$; **b** $\alpha = -0.5$

(I) For both cases $\alpha = +0.5$ and $\alpha = -0.5$, the FGM dispersion curves vary considerably in the whole frequency range $\omega \in (0; \infty)$.

(II) For *homogenized* plates at small frequencies $\omega \to 0$, the corresponding phase velocities coincide with the second limiting wave velocity: $c_{2,\mathrm{lim}} = \sqrt{E_{\mathrm{hom}}/\rho}$, see [13]; thus $c_{2,\mathrm{lim}} \approx 0.892$ at $\alpha = +0.5$ and $c_{2,\mathrm{lim}} \approx 0.454$ at $\alpha = -0.5$.

(III) For *homogenized* plates at high frequencies $\omega \to \infty$, the corresponding phase velocities coincide with the Rayleigh wave velocities $c_R \approx 0.518$ at $\alpha = +0.5$ and $c_R \approx 0.264$ at $\alpha = -0.5$.

(IV) For FGM plates at high frequencies $\omega \to \infty$, the corresponding phase velocities are very close to the Rayleigh wave velocities that relate to physical properties of the outer layers: at $\alpha = +0.5$, according to Eq. (5.1), $E(\pm h) \approx 0.885$ which yields $c_R \approx 0.547$, and at $\alpha = -0.5$, according to Eq. (5.1), $E(\pm h) \approx 0.114$ which yields $c_R \approx 0.197$.

(V) For the considered FGM plates, frequency values of nonexistence of symmetric fundamental modes were not observed.

Generally, as the corresponding plots in Fig. 3 show for the considered FGM plates, homogenization leads to a substantial discrepancy in the dispersion curves in the whole frequency range $\omega \in (0; \infty)$.

6 Conclusions

Propagation of harmonic Lamb waves in plates made of functionally graded materials (FGM) with transverse inhomogeneity is studied by the modified Cauchy six-dimensional formalism. For arbitrary transverse inhomogeneity, a closed-form dispersion equation is derived.

Dispersion curves for FGM isotropic plates with different kinds of exponential inhomogeneity are obtained and compared with those for homogenized isotropic plates, revealing a substantial discrepancy in the shape of the corresponding dispersion curves.

For the considered inhomogeneities, no frequency values were found at which nonexistence of the symmetric fundamental Lamb wave modes could occur.

References

1. Liu, G.R., Tani, J., Ohyoshi, T.: Lamb waves in a functionally gradient material plates and its transient response. Part 1: Theory; Part 2: calculation result. Trans. Jpn. Soc. Mech. Eng. **57A**, 131–42 (1991)
2. Koizumi, M.: The concept of FGM. Ceram. Trans. Funct. Gradient Mater. **34**, 3–10 (1993)
3. Liu, G.R., Tani, J.: Surface waves in functionally gradient piezoelectric plates. Trans. ASME. **116**, 440–448 (1994)
4. Miyamoto, Y., Kaysser, W.A., Brain, B.H., Kawasaki, A., Ford, R.G.: Functionally Graded Materials. Academic Publishers, Kluwer (1999)
5. Han, X., Liu, G.R., Lam, K.Y., Ohyoshi, T.: A quadratic layer element for analyzing stress waves in FGMs and its application in material characterization. J. Sound Vib. **236**, 307–321 (2000)
6. Vlasie, V., Rousseau, M.: Guide modes in a plane elastic layer with gradually continuous acoustic properties. NDT&E Int. **37**, 633–644 (2004)

7. Baron, C., Naili, S.: Propagation of elastic waves in a fluid-loaded anisotropic functionally graded waveguide: application to ultrasound characterization. J. Acoust. Soc. Am. **127**(3), 1307–1317 (2010)
8. Amor, M.B., Ghozlen, M.H.B.: Lamb waves propagation in functionally graded piezoelectric materials by Peano-series method. Ultrasonics **4905**, 1–5 (2014)
9. Nanda, N., Kapuria, S.: Spectral finite element for wave propagation analysis of laminated composite curved beams using classical and first order shear deformation theories. Compos. Struct. **132**, 310–320 (2015)
10. Chao, Xu, Zexing, Yu.: Numerical simulation of elastic wave propagation in functionally graded cylinders using time-domain spectral finite element method. Adv. Mech. Eng. **9**(11), 1–17 (2017)
11. Lefebvre, J.E., et al.: Acoustic wave propagation in continuous functionally graded plates: an extension of the Legendre polynomial approach. IEEE T Ultrason. Ferr. **48**, 1332–1340 (2001)
12. Qian, Z.H., Jin, F., Wang, Z.K., Kishimoto, K.: Transverse surface waves on a piezoelectric material carrying a functionally graded layer of finite thickness. Int. J. Eng. Sci. **45**, 455–466 (2007)
13. Kuznetsov, S.V.: Lamb waves in anisotropic plates (Review). Acoust. Phys. **60**(1), 95–103 (2014)
14. Djeran-Maigre, I., Kuznetsov, S.V.: Soliton-like Lamb waves in layered media. In: Vila, R.P. (ed.) Waves in Fluids and Solids, pp. 53–68. IntechOpen, Maidenhead (2011)